Binding of distinct substrate conformations enables hydroxylation of remote sites in thaxtomin D by cytochrome P450 TxtC

Lona M. Alkhalaf[§‡], Sarah M. Barry[§†‡], Dean Rea[¥], Angelo Gallo[§], Daniel Griffiths[§Ψ], Józef R. Lewandowski[§], Vilmos Fulop[¥] and Gregory L. Challis[§*]

§ Department of Chemistry, University of Warwick, Coventry, CV4 7AL, UK; ¥ School of Life Sciences, University of Warwick, Coventry, CV4 7AL, UK

ABSTRACT: Cytochromes P450 (CYPs) catalyze various oxidative transformations in drug metabolism, xenobiotic degradation and natural product biosynthesis. Here we report biochemical, structural and theoretical studies of TxtC, an unusual bifunctional CYP involved in the biosynthesis of the EPA-approved herbicide thaxtomin A. TxtC was shown to hydroxylate two remote sites within the Phe residue of its diketopiperazine substrate thaxtomin D. The reactions follow a preferred order, with hydroxylation of the α-carbon preceding functionalization of the phenyl group. To illuminate the molecular basis for remote site functionalization, X-ray crystal structures of TxtC in complex with the substrate and monohydroxylated intermediate were determined. Electron density corresponding to a diatomic molecule (probably dioxygen) was sandwiched between the heme iron atom and Thr237 in the TxtC-intermediate structure, providing insight into the mechanism for conversion of the ferrous-dioxygen complex into the reactive ferryl intermediate. The substrate and monohydroxylated intermediate adopted similar conformations in the active site, with the π-face of the phenyl group positioned over the heme iron atom. Docking simulations reproduced this observation and identified a second, energetically similar but conformationally-distinct binding mode in which the α-hydrogen of the Phe residue is positioned over the heme prosthetic group. Molecular dynamics simulations confirmed that the α-hydrogen is sufficiently close to the ferryl oxygen atom to be extracted by it and indicated that the two substrate conformations cannot readily interconvert in the active site. These results indicate that TxtC is able to hydroxylate two spatially remote sites by binding distinct conformations of the substrate and monohydroxylated intermediate.

Introduction

Cytochromes P450 (CYPs) are versatile monoxygenases that employ a heme prosthetic group ligated to a conserved active site Cys residue and an electron transfer protein partner to activate molecular oxygen.[1] The resulting ferryl (Fe^{IV}=O) reactive intermediate effects a wide range of oxidative transformations. These enzymes frequently play key roles in the biosynthesis of microbial natural products, including the assembly of non-proteinogenic amino acid precursors, and the catalysis of diverse on and post-assembly line tailoring reactions.[2-6] A handful of CYPs, all of which tailor the products of polyketide synthase assembly lines, have been shown to be multifunctional[7]. These enzymes catalyze the sequential oxidation of two or three proximal carbon centers and in most cases come from Actinobacteria (Figure 1), although fungal examples are also known. Structural studies of two such enzymes have indicated that only small changes in the positioning of the substrate relative to the heme prosthetic group are required to achieve the successive oxidation reactions, because the atoms undergoing functionalization are positioned adjacent to each other.[8-10]

Several plant-pathogenic Actinobacteria, including *Streptomyces acidiscabies*, *Streptomyces turgidscabies* and *Streptomyces scabies*, produce thaxtomins, a family of phytotoxic diketopiperazines that inhibit cellulose biosynthesis in expanding plant tissues.[11] *S. scabies* causes common scab in potatoes and other economically important crops,[12] and thaxtomin A **1** has been approved by the EPA for use as an herbicide (registration number: 84059-12), although it has yet to reach the market. Five genes within a mobile pathogenicity island are responsible for thaxtomin biosynthesis in *S. scabies* 87.22 (Figure 2).[11] The *txtA* and *txtB* genes encode a dimodular nonribosomal peptide synthetase (NRPS) that assembles thaxtomin D **2** from L-Phe, L-4-nitrotryptophan and two units of *S*-adenosyl-L-methionine (SAM) (Figure 2).[13] The *txtE* gene encodes an unusual CYP that catalyzes regiospecific nitration of L-Trp at the 4-position of the indole using O_2 and NO, which is generated from L-Arg by the nitric oxide synthase encoded by *txtD*.[3, 14] Gene deletion experiments have implicated *txtC*, which is also predicted to encode a CYP, in the conversion of thaxtomin D **2** to thaxtomin A **1**.[15] However, direct evidence for hydroxylation of both the Phe α-carbon and the phenyl group in thaxtomin D **2** by TxtC is lacking. Moreover, catalysis of both these reactions by a single CYP could be considered somewhat remarkable, given that the resulting hydroxyl groups are separated by almost 7 Å in the X-ray crystal structure of thaxtomin A **1**.[16]

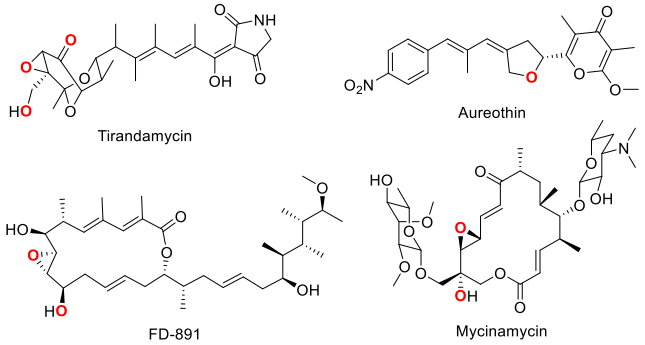

Figure 1: Structures of actinobacterial polyketides assembled by multifunctional CYPs. The oxygen atoms introduced by the CYP in each case are highlighted in red.

Here we report the overproduction in *Escherichia coli* and purification of TxtC, and show that it catalyzes sequential hydroxylation of the Phe α-carbon and the phenyl group in thaxtomin D **2**. X-ray crystal structures of TxtC in complex with thaxtomin D **2** and thaxtomin B **3** (the monohydroxylated intermediate), combined with docking and molecular dynamics simulations, suggest that the enzyme catalyzes functionalization of these two spatially remote carbon centers by binding distinct conformational states of its two substrates.

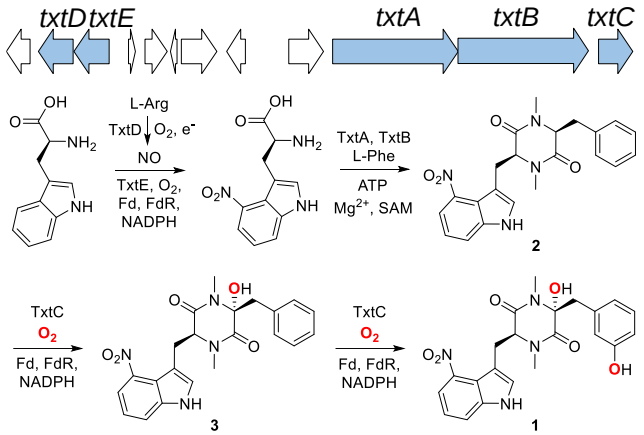

Figure 2: Organization of the mobile pathogenicity island in *S. scabies* 87.22 responsible for thaxtomin biosynthesis (biosynthetic genes are shaded blue) and proposed pathway for assembly of thaxtomin A **1** (Fd = ferredoxin, FdR = Fd reductase).

Results and discussion

TxtC from *Streptomyces acidiscabies* 84.104 has previously been overproduced in *E. coli*, but UV-Vis spectroscopic analysis of the purified protein indicated that it exists in the catalytically inactive P420 form.[15] We cloned *txtC* from *S. scabies* 87.22 and overexpressed it in *E. coli* as an *N*-terminal His_6-fusion. The resulting protein was soluble and was readily purified from cell lysate using Ni-NTA chromatography (Figure S1). The identity of the purified protein was confirmed by peptide mass fingerprinting and gel filtration chromatography indicated that it is monomeric (Figure S2). Absorbance maxima at 419 and 450 nm were observed for the ferric and ferrous-CO forms of the protein, respectively, confirming that this CYP is produced in a catalytically active form (Figure S3).

A mutant of *S. acidiscabies* 84.104 in which *txtC* has been disrupted accumulates thaxtomin D **2**, suggesting that this metabolite could be a substrate for TxtC.[15] To test this hypothesis, we incubated purified recombinant TxtC with thaxtomin D **2**, isolated from the *txtC* mutant, NADPH, and spinach ferredoxin/ferredoxin reductase (required to transfer electrons form NADPH to the heme prosthetic group of CYPs). LC-MS analysis of the reaction mixture identified two major products, giving rise to ions with *m/z* values 16 and 32 Da higher than the substrate. Semi-preparative HPLC purification of these products from a scaled-up reaction and ESI-Q-TOF-MS analysis showed that the molecular formula of the higher molecular weight compound corresponds to that for thaxtomin A **1**, whereas the lower molecular weight compound has the same molecular formula as thaxtomin B **3** (Figure S4). ^{1}H NMR spectroscopic comparisons of the purified products with authentic standards of thaxtomins A and B isolated from *S. acidiscabies* 84.104 confirmed these structural assignments (see supporting information). In addition to thaxtomin A **1**, small amounts of two additional products with molecular weights 32 Da higher than the substrate were observed in the TxtC-catalyzed reaction. These compounds could not be purified in sufficient quantities to permit ^{1}H NMR spectroscopic analysis. However, ESI-Q-TOF-MS showed that they have the same molecular formulae as thaxtomin A **1** (see supporting information). These are likely isomers of thaxtomin A **1**, in which the aromatic hydroxyl susbtituent is situated *ortho* or *para* to the methylene group, because such compounds are known to be biosynthesized in small amounts by thaxtomin-producing *Streptomyces* species. To substantiate this hypothesis, we purified an authentic standard of the *o*-isomer from *S. acidiscabies* 84.104, confirmed its identity by HRMS and ^{1}H NMR spectroscopy, and showed that its retention time is identical to one of the minor dihydroxylated products of the enzymatic reaction (Figure S4). By a process of elimination, we assigned the other dihydroxylated product of the enzymatic reaction as the *p*-isomer. All four hydroxylated products were absent from control reactions in which the enzyme was inactivated by boiling, or from which the ferredoxin, ferredoxin reductase or NADPH were omitted (Figure S5).

To investigate whether the TxtC-catalyzed hydroxylation reactions follow a defined order, the disappearance of the substrate and the formation of mono- and dihydroxylated products was monitored over a 60 minute period (Figure 3). Within 5 minutes, most of the substrate is consumed and thaxtomin B **3** (along with a small amount of another monohydroxylated species), thaxtomin A **1** and its *o*-isomer are formed. Over the next 55 minutes, the amount of thaxtomin B **3** in the mixture steadily decreases and a concomitant increase in the quantities of thaxtomin A **1** and its *o*/*p*-isomers is observed. These data imply that thaxtomin B **3** is the main intermediate in the TxtC-catalyzed

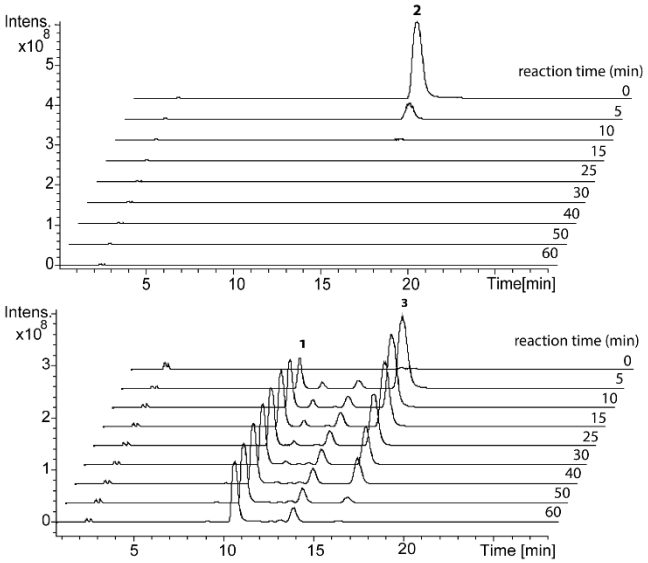

Figure 3: Extracted ion chromatograms (EICs) from LC-MS analyses of TxtC-catalyzed hydroxylation of thaxtomin D **2** showing that thaxtomin B **3** is an intermediate in its conversion to thaxtomin A **1**. Top: EIC at *m/z* = 429 corresponding to $[M+Na]^+$ for **2**. Bottom: EIC at *m/z* = 445 and 461 corresponding to $[M+Na]^+$ for **1** and **3**, respectively. The *p*- and *o*-isomers of **1** have retention times of ~10 and ~14 minutes, respectively. The compound with a retention time of ~12 minutes that forms transiently in small quantities during the course of the reaction has an *m/z* corresponding to an alternative monohydroxylated intermediate.

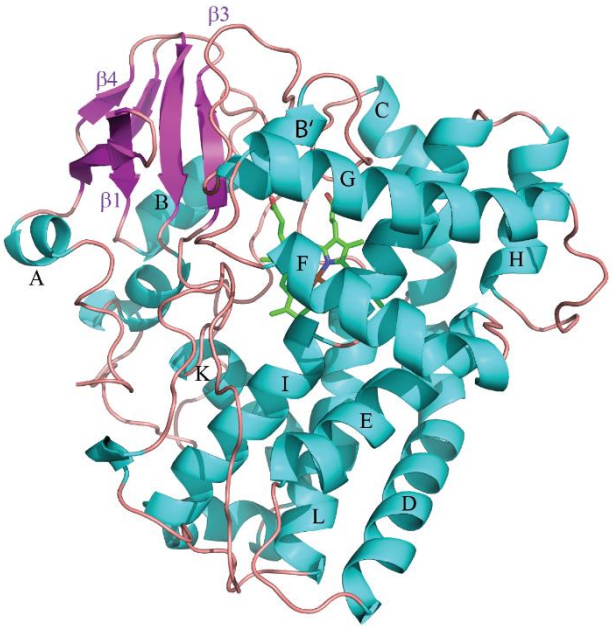

Figure 4: Overall structure of the TxtC-thaxtomin D **2** complex highlighting the location of the heme prosthetic group (in green). The α-helix and β-sheet secondary structure elements are labeled according to standard CYP nomenclature.

dihydroxylation of thaxtomin D **2**. Incubation of thaxtomin B **3** with TxtC, NADPH and spinach ferredoxin/ferrodoxin reductase resulted in the formation of thaxtomin A **1** as well as small quantities of its *o*/*p*-isomers, consistent with this hypothesis (Figure S4).

Taken together our data unambiguously show that TxtC catalyzes the final two steps in thaxtomin A **1** biosynthesis. They further suggest that these reactions occur in a preferred order, with hydroxylation of the Phe α-carbon to give thaxtomin B **3** occurring first, followed by functionalization of the phenyl group to give thaxtomin A **1**, along with small quantities of its *o* and *p*-isomers. The fact that thaxtomin B **3**, but no isomers in which the aromatic ring of the Phe residue is hydroxylated instead of its α-carbon are produced by thaxtomin-producing *Streptomyces* species further supports this conclusion.

To develop an understanding of a how a single CYP is able to catalyze the successive hydroxylation of two spatially remote sites in a single molecule, TxtC was co-crystallized with its substrate thaxtomin D **2** and the monohydroxylated intermediate thaxtomin B **3**. The X-ray structures of these complexes were solved to 2.8 and 1.7 Å, respectively, by molecular replacement using MoxA from *Nonomuraea recticatnina* (PDB ID: 2Z36) as a template. Attempts to crystallize TxtC in the absence of substrate were unsuccessful, suggesting that the unliganded enzyme has a high degree of conformational flexibility. The overall structure of TxtC is very similar to that of other well-characterized bacterial CYPs, such as P450cam (Figure 4).[17] Both complexes were found to adopt an essentially identical closed conformation in which the substrates are sequestered from solvent.

In the structure of the TxtC-thaxtomin B complex, the 4-nitroindole moiety of the substrate is embedded in a pocket lined by the side chains of predominantly hydrophobic residues (Leu74, Pro82, Val84, Phe182, Leu228, Met229 and Val232). On one side of this pocket, the carboxylate side chain of Glu69 forms a hydrogen bond with the N-H group of the indole (Figure 5A). Two further polar contacts between the substrate and the enzyme are mediated by water molecules. One of these forms hydrogen bonds with the side chain of Thr385, and the carbonyl group of the Phe residue in the substrate (Figure 5A). The other sits in close proximity to the carbonyl group of 4-nitrotryptophan and one of the carboxylate groups of the active site heme (Figure 5A). Together these two water molecules anchor the diketopiperazine of thaxtomin B **3** in the active site, positioning the π-face of the phenyl group in this monohydroxylated intermediate over the heme prosthetic group (Figures 5A and S10). Electron density corresponding to a diatomic molecule was also found in close proximity to the heme iron atom with 100% occupancy (Figure 5A). This is likely dioxygen, which binds to the active site as a result of heme photoreduction during X-ray data collection, as reported previously for P450cam.[18, 19] The distal end of this diatomic molecule (relative to the heme) hydrogen bonds to the side chain of Thr237, a highly conserved residue in CYPs that has been shown to be important for catalysis.[20, 21] A further water molecule sits within H-bonding distance of the Thr237 hydroxyl group, the distal end of the diatomic molecule, and the water molecule that interacts with the Thr385 side chain (Figure 5A).

The phenyl group of the substrate is positioned close to the proximal end of the heme-associated diatomic molecule in the TxtC-thaxtomin B **3** structure (Figure 5A). To investigate whether this binding mode permits hydroxylation of the phenyl group, we replaced the heme and its associated diatomic molecule with compound I (heme oxyferryl complex) and carried out molecular dynamics (MD) simulations. The results of these simulations show that all five unsubstituted carbon atoms of the phenyl group are able to approach the ferryl oxygen to within ~3.2 Å (Table 1), explaining why a mixture of *o*-, *m*- and *p*-hydroxylated products is formed. The average and minimum distances of the unsubstituted carbon atoms from the ferryl oxygen are smallest for the *o*-positions and largest for the *p*-positions (Table 1), although the differences are small and may not be relevant to the observed preference for *m*-hydroxylation. Nevertheless, it is possible that thaxtomin A **1** results only partially from direct attack of the ferryl oxygen at the *m*-position (Figure 6). The intermediate resulting from attack of the ferryl oxygen at the *o*-position could undergo 1,3-elimination to form an arene oxide that rearranges via an "NIH shift" to form the *m*-product (Figure 6). While the involvement of arene oxides in CYP-catalyzed aromatic hydroxylation reactions has been questioned on theoretical grounds,[22] such a species has recently been implicated as an intermediate in the P450cam-catalysed oxidation of *t*-butyl-benzene.[23]

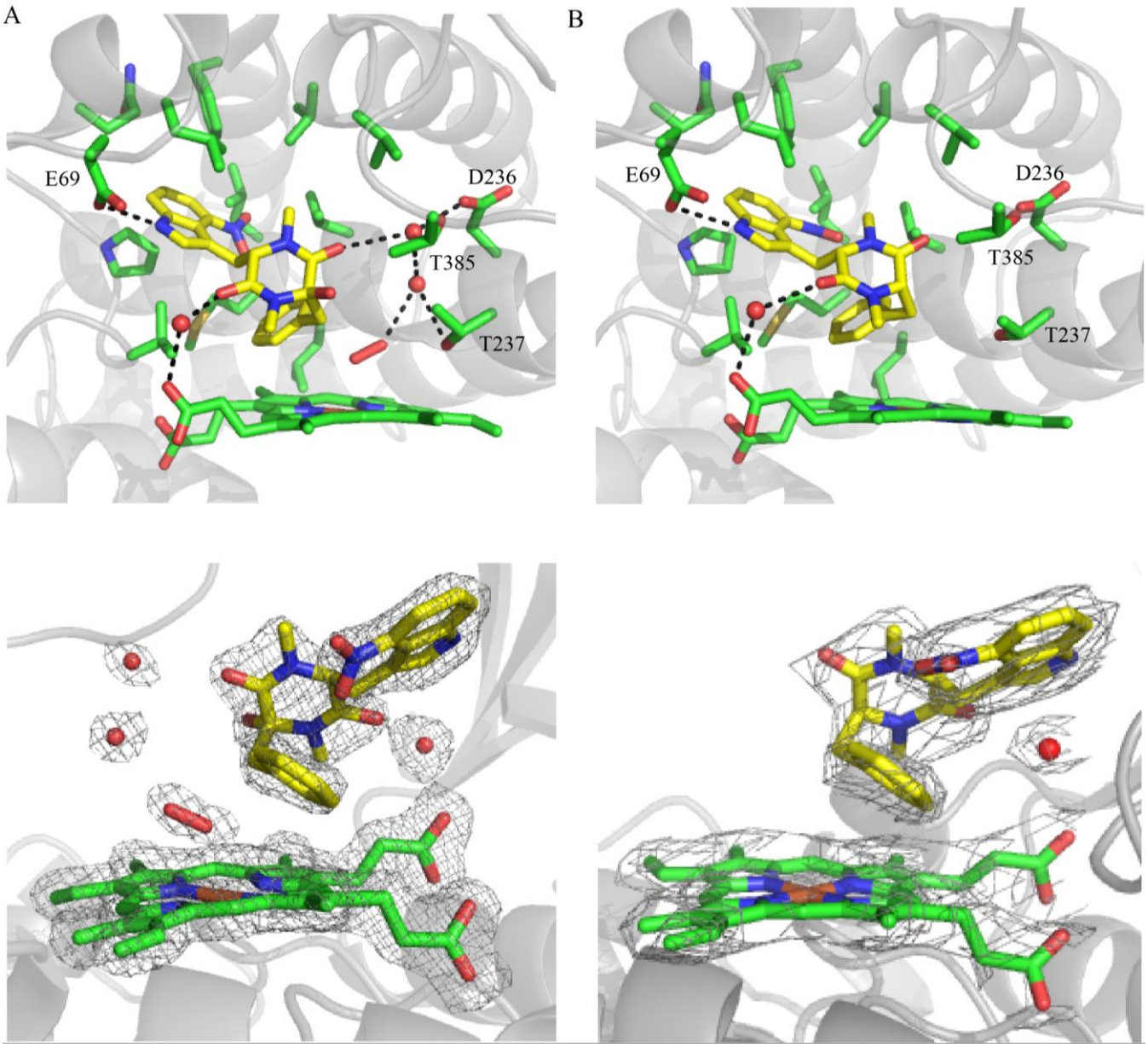

Figure 5: (A) Active site in the TxtC-thaxtomin B **3** complex (PDB ID: 6F0C), highlighting key hydrogen bonding interactions between the substrate, protein and active site water molecules as dashed lines (top) and showing the electron density for the substrate, heme prosthetic group, diatomic molecule and three ordered water molecules (bottom). (B) Active site in the TxtC-thaxtomin D (**2**) complex (PDB ID: 6F0B) highlighting hydrogen bonds as dashed lines (top) and showing the electron density for the substrate, heme prosthetic group, and single ordered water molecule (bottom). Both $2F_0$-F_c electron density maps were contoured at 1σ with the bound ligand atoms omitted from the density calculations.

Table 1: Minimum, maximum and average distances (Å) between the ferryl oxygen and the unsubstituted carbon atoms of the thaxtomin B **3** phenyl group observed in MD simulations.

position	minimum	maximum	average
o/o'	2.81/2.83	4.58/4.91	3.61/3.75
m/m'	3.19/3.13	5.35/5.95	4.28/4.64
p	3.23	5.94	4.67

The structure of the TxtC-thaxtomin B complex also suggests a mechanism for the transfer of protons from bulk solvent to the ferrous dioxygen complex via Asp236, which forms an interface between the active site and a water filled exterior pocket (Figure 7). Two water molecules connect the distal end of the heme-associated diatomic molecule to the carboxylate side chain of Asp236 (Figure 5A) and are thus proposed to function as a proton relay (Figure 7). A similar mechanism, in which the corresponding aspartate residue (Asp251) and a single active site water molecule participate in proton delivery during the rate limiting step of O-O bond cleavage, has been proposed for P450cam.[24] Consistent with this hypothesis, a D251N mutant was reported to be much less active than the wild type enzyme.[24] More recently, the binding of the electron donor putidaredoxin to P450cam has been shown to break a salt bridge between Lys178/Arg186 and Asp251, allowing the side chain of the latter to pick up a proton from the bulk solvent and deliver it to the active site.[25, 26] This indicates that reduction of the ferrous-dioxygen intermediate and protonation of the resulting ferric peroxide are tightly coupled. TxtC contains an analogous salt bridge

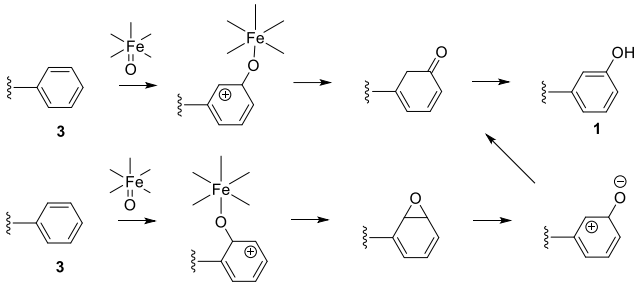

Figure 6: Possible mechanisms for TxtC-catalyzed conversion of thaxtomin B **3** to thaxtomin A **1**.

between Arg380 and Asp236, suggesting that it may employ a similar mechanism.

Surprisingly, the substrate in the TxtC-thaxtomin D structure is bound in a very similar conformation to the monohydroxylated intermediate in the TxtC-thaxtomin B structure (Figures 5B and S10). In this conformation, the α-hydrogen atom of the Phe residue points away from the heme and appears to be too far away from the iron center to be extracted by the ferryl intermediate. Indeed, we could find no frames in MD simulations of this structure in which this hydrogen atom adopts a near attack conformation (a distance of >3.5 Å between the hydrogen atom and the ferryl oxygen and a C-H-O bond angle of 180 ± 45º; see Table S9).[27] Moreover, no electron density corresponding to either the diatomic molecule, or the two water molecules that connect its distal end to Asp236 and Thr385 is observed in the TxtC-thaxtomin D structure (Figure 5B). As a consequence, the distance between the substrate and the I-helix (containing Asp236 and Thr237) decreases relative to the TxtC-thaxtomin B structure (Figure S11). In contrast, the water molecule sandwiched between the 4-nitrotryptophan carbonyl and heme carboxylate groups adopts a very similar position in both structures. The substrate binding mode observed in the TxtC-thaxtomin D structure thus appears to disfavor formation of a ferrous-dioxygen complex, and the substrate must bind in a different conformation to permit Phe α-carbon hydroxylation.

To investigate whether thaxtomin D **2** can bind to TxtC in different conformational states, docking simulations were conducted using SwissDock.[28] The results of these simulations predict that the active site of the enzyme can accommodate three distinct conformational states of thaxtomin D, which have predicted Gibbs free energies of binding within 0.2 kcal of each other (Figure S12). In all three of these states, the 4-nitroindole moiety is bound in the same position as that observed in the TxtC-thaxtomin D structure. Moreover, in one of the states the phenyl group of the substrate is positioned above the heme iron atom, accurately recapitulating the experimentally-observed substrate binding orientation in the TxtC-thaxtomin D structure (Figure S12). In another state, arising from rotation about the β-γ bond of the 4-nitrotryptophan residue, the diketopiperazine is flipped such that the phenyl group is pointing towards the roof of the active site (Figures 8 and S12). This positions the α-hydrogen atom of the Phe residue in close proximity to the heme iron atom and it was found to adopt a near attack conformation in 6% of the frames in MD simulations (Figures 8 and Table S9). No interconversion between the different substrate binding orientations was observed in the MD simulations. Close examination of the substrate binding site in TxtC indicates that a steric clash between the side chain of the Phe residue in the substrate and the heme / residues 231-236 in the I helix prevents this. The switch in conformation of the monohydroxylated intermediate that enables hydroxylation of its phenyl group thus appears to require release from the active site of TxtC.

Conclusion

Our work demonstrates that TxtC is an unusual CYP capable of oxidizing two spatially remote sites in thaxtomin D **2**. These hydroxylation reactions proceed in a preferred order with functionalization of the Phe α-carbon preceding oxidation of the phenyl group. X-ray crystallographic analysis of TxtC with the mono-hydroxylated intermediate thaxtomin B **3** bound in its active site positions the π-face of the phenyl group in this substrate over the iron atom of the heme prosthetic group, such that hydroxylation can occur. MD simulations of the TxtC-compound I-thaxtomin B complex confirmed that all five of the unsubstituted carbon atoms in the phenyl group are able to approach the ferryl oxygen atom sufficiently close to react. It appears that the predominant *m*-substituted product of the aromatic hydroxylation reaction may be formed by a combination of direct attack of the ferryl oxygen at the *m*-position and attack at the *o*-position, followed by rearrangement to the *m*-product via an arene oxide intermediate. The TxtC-thaxtomin B structure also revealed that a network of hydrogen bonds connects a heme iron-bound diatomic molecule (probably dioxygen), via a pair of active site water molecules, to a conserved aspartate residue, which is proposed to shuttle protons from the bulk solvent into the active site. This enables protonation of the ferric-peroxide intermediate leading to formation of the reactive ferryl species. Surprisingly, in the X-ray crystal structure of the TxtC-thaxtomin D complex thaxtomin D **2** was bound in the same orientation as thaxtomin B **3**. MD simulations confirmed that the α-H of the Phe residue cannot be extracted by the ferryl

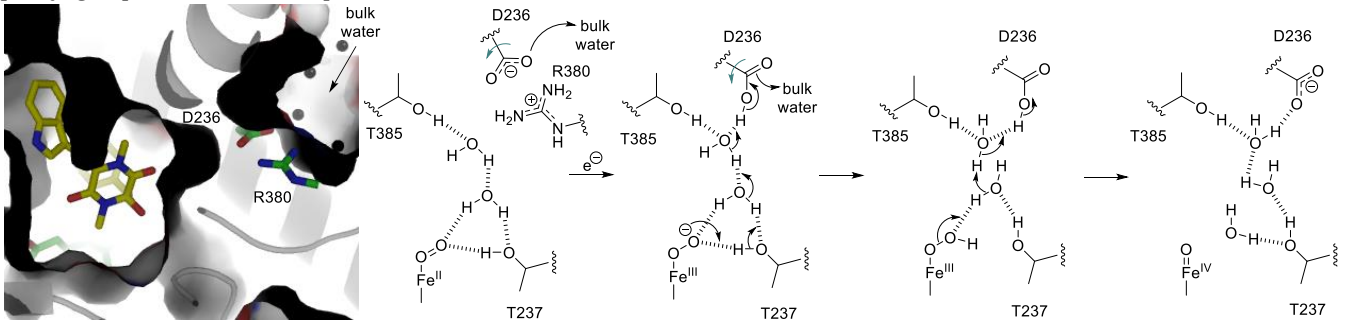

Figure 7. Proposed mechanism for transfer of protons from bulk solvent to the ferric peroxide intermediate in TxtC, via two active site water molecules and Asp236. The grey arrows indicate that a 180° rotation of the C_β-C_γ bond in Asp236 is required to deliver the protons picked up from the bulk solvent into the active site. The juxtaposition of Asp236 and Arg380 between the substrate binding pocket and a water-filled exterior pocket is illustrated on the left.

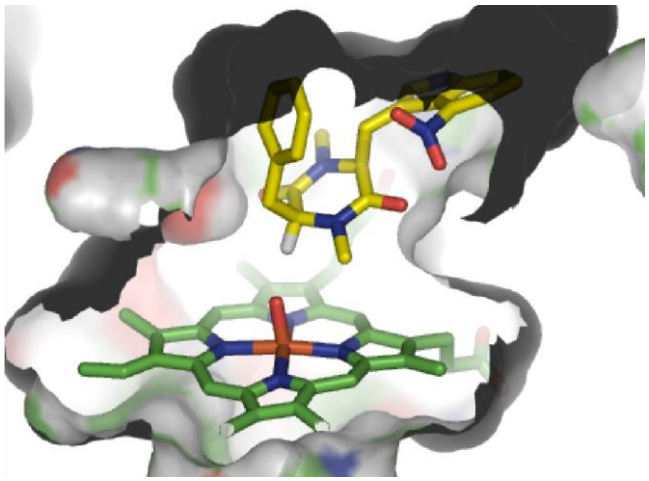

Figure 8: Example of a near attack conformation observed in MD simulations of TxtC containing the compound I complex and thaxtomin D **2** bound in the "flipped" orientation with the phenyl group pointing towards the roof of the active site. This positions the α-hydrogen atom of the Phe residue sufficiently close to the ferryl oxygen to be extracted by it.

intermediate when thaxtomin D is bound in this orientation. Docking simulations recapitulated this binding mode, but also revealed an energetically similar yet conformationally-distinct substrate binding orientation that places the Phe α-hydrogen atom close to heme iron atom. MD simulations confirmed that this hydrogen atom can get close enough to the ferryl oxygen to be abstracted by it, when the substrate is bound in this orientation. Overall, our data indicate that the main reaction path of TxtC involves hydroxylation of first the Phe α-carbon and then the phenyl group of thaxtomin D **2** by binding distinct conformational states of the substrate and mono-hydroxylated intermediate, contributing new insights into the mechanisms employed by multifunctional CYPs for the functionalization of spatially remote carbon atoms.

ASSOCIATED CONTENT

Supporting Information: Experimental procedures, SDS-PAGE analysis of His6-TxtC expression and purification, the results of the enzyme activity assays, spectroscopic characterization data, and details of the docking and MD simulations are included in the supporting information. This material is available free of charge via the Internet at http://pubs.acs.org. The coordinates of the TxtC-thaxtomin D complex (Accession No. 6F0B) and the TxtC-thaxtomin B complex (Accession No. 6F0C) have been deposited in the Protein Data Bank.

AUTHOR INFORMATION

Corresponding Author

* G.L.Challis@warwick.ac.uk

Present Addresses

†Department of Chemistry, Kings College London, Strand, London, WC2R 2LS
Ψ Department of Biochemistry and Molecular Biology Monash University, Clayton VIC 3800, Australia

Author Contributions

‡These authors contributed equally.

ACKNOWLEDGMENT

This work was supported by grants from the UK BBSRC (Grant Ref. BB/H006281/1). We thank Rose Loria (Cornell University) for providing the *txtC* mutant and wild type *S. acidiscabies*. The Bruker MaXis mass spectrometer used in this research was obtained, through Birmingham Science City: Innovative Uses for Advanced Materials in the Modern World (West Midlands Centre for Advanced Materials Project 2), with support from Advantage West Midlands (AWM) and part funded by the European Regional Development Fund (ERDF). Crystallographic data were collected on beam line I24 at the Diamond Light Source, UK and we acknowledge the support of the beam line scientists.

REFERENCES

1) Denisov, I. J.; Makris,T. M.; Sligar, S. G.; Schlichting, I. *Chem. Rev*. **2005**, *105*, 2253-2277.

2) Podust, L. M.; Sherman D. H. *Nat. Prod. Rep*. **2012**, *10*, 1251-1266.

3) Barry, S. M.; Kers, J. A.; Johnson, E. R.; Song, L.; Aston, P. R.; Patel, B.; Krasnoff, S. B.; Gibson, D. M.; Loria, R.; Challis, G. L. *Nat Chem Biol.* **2012**, *8*, 814-816.

4) Song, L.; Laureti L.; Corre, C.; Leblond, P.; Aigle, B.; Challis, G. L; *J. Antibiot.* **2014**, *67*, 71-76.

5) Zabala, D.; Cartwright, J.W.; Roberts, D.M.; Law, B.J.C.; Song, L.; Samborskyy M.; Leadlay, P.F.; Micklefield J.; Challis, G.L. *J. Am. Chem. Soc*. **2016**, *137*, 4342-4345.

6) Haslinger, K.; Peschke, M.; Brieke, C.; Maximowitch, E.; Cryle, M. J. *Nature*, **2015**, *521*, 105-109.

7) Cochrane, R. V. K.; Vederas, J. C. *Acc. Chem. Res.* **2014**, *47*, 3148–3161.

8) Li, S.; Tietz, D. R.; Rutaganira, F. U.; Kells, P. M.; Anzai, Y.; Kato, F.; Pochapsky, T. C.; Sherman, D. H.; Podust, L. M. *J. Biol. Chem.* **2012**, *287*, 37880−37890.

9) Tietz, D. R.; Podust, L. M.; Sherman, D. H.; Pochapsky, T. C. *Biochemistry*, **2017**, *56*, 2701-2714.

10) Zocher, G.; Richter, M. E. A.; Mueller, U.; Hertweck, C. *J. Am. Chem. Soc*., **2011**, *133*, 2292−2302.

11) King, R. R..; Calhoun, L.A. *Phytochemistry*, **2009**, *70*, 833-841.

12) Lambert, D.H., Loria, R. *Int. J. Syst. Bacteriol.* **1989**, *39*, 387–392.

13) Johnson, E. G.; Krasnoff, S. G.; Bignell, D. R. D.; Chung, W. C.; Tao, T.; Parry, R. J.; Loria, R.; Gibson, D. M.; *Mol. Microbiol*. **2009**, *73*, 409-418.

14) Kers, J.A.; Wach, M. J.; Krasnoff, S. B.; Widom, J.; Cameron, K. D.; Bukkhalid, R. A.; Gibson, D. M.; Crane, B. R.; Loria, R. *Nature*, **2004**, *429*, 79-82

15) Healy, F. G.; Krasnoff, S. B.; Wach, M.; Gibson, D. M.; Loria, R. *J. Bacteriol.* **2002**, *184*, 2019-2029.

16) Bourgault, J. P.; Maddirala, A. R.; Andreana, P. R. *Org. Biomol. Chem*. **2014**, 12, 8125-8127

17) Poulos, T.; Finzel, B.C.; Howard, A.J. *J. Mol. Biol.* **1987**, *195*, 687-700.

18) Beitlich, T.; Kuhnell, K.; Schluze-Briese, C.; Shoeman, R.L.; Schlichting, I., *J. Synchrotron Rad.* **2007**, *14*, 11–23.

19) Schlichting, I.; Berendzen, J.; Chu, K.; Stock, A.M.; Maves, S.A.; Benson, D.E.; Sweet, R.M.; Ringe, D.; Petsko, G.A.; Sligar, S.G. *Science*, **2000**, *287*, 1615-1622.

20) Martinis, S. A.; Atkins, W. M.; Stayton, P.S.; Sligar, S. G. *J. Am. Chem. Soc*. **1989**, *30*, 11420-11429.

21) Raag, R.; Martinis, S. A.; Sligar, S. G.; Poulos, T. L. *Biochemistry*, **1991**, *30*, 11420-11429.

22) deVisser, S.P.; Shaik, S. *J. Am. Chem. Soc.* **2003**, *125*, 7413-7424.

23) Stok, J. E.; Chow, S.; Kresenke, E. H.; Soto, C. F.; Matyas, C.; Poirier, R. A.; Williams, C. M.; de Voss, J. J. *Chem. Eur. J.* **2016**, *22*, 4408-4412.

24) Gerber, N.C.; Sligar, S.G., *J. Biol. Chem.*, **1994**, *269*, 4260-4266.

25) Tripathi, S.; Li, H.; Poulos, T. *Science*, **2013**, 340, 1227-1230.

26) Batabyal, D.; Richards, L.S.; Poulos, T.L. *J. Am. Chem. Soc*. **2017**, *139*, 13193-13199.

27) Eichler, A.; Gricman, L.; Herter, S.; Kelly, P.; Turner, N.; Pleiss, J.; Flitsch, S. *ChemBioChem*, **2015**, *5*, 426–432.

28) Grosdidier, A.; Zoete, V.; Michielin, O. *Nucleic Acids Res.* **2011**, *39*, 270-277.

Table of contents graphic